

Automated Verification of Potential GPS Signal-In-Space Anomalies Using Ground Observation Data

Liang Heng, Grace Xingxin Gao, Todd Walter, and Per Enge

GPS Research Laboratory

Department of Aeronautics & Astronautics

Stanford University

Stanford, CA 94305, USA

Email: {lheng, gracegao, twalter, penge}@stanford.edu

Abstract—For the Global Positioning System (GPS), signal-in-space (SIS) user range error (URE), the pseudorange inaccuracy attributable to the ground control and the space vehicles, is one of the major error sources affecting positioning accuracy and integrity. As SIS anomalies occur occasionally and UREs of tens of meters or even more have been observed, knowledge of the SIS anomalies in history has a great importance for not only assessing the general GPS SIS performance but also developing next generation GNSS integrity monitoring systems.

Our prior work has identified many potential GPS SIS anomalies in the last decade by comparing broadcast ephemerides and clocks with precise ones. However, this approach is prone to false anomalies. In this paper, we develop an automated process to verify previously identified GPS SIS anomalies using the ground observation data from the International GNSS Service (IGS).

For each potential GPS SIS anomaly, our process first determines 10–32 preferred IGS stations, and retrieves their observation and navigation data. Then, the SIS UREs are computed by deducting non-SIS UREs, such as tropospheric delays, ionospheric delays, and multipaths, from total UREs. Finally, the observation data from each IGS station generate a decision among “anomalous,” “normal,” and “untracked;” these independent decisions are combined to determine if the potential anomaly is true, false, untracked, or paradoxical.

We apply this process to the 31 potential SIS anomalies found during the past eight years. The results show that 26 potential SIS anomalies are true, 1 is false, and 4 are untracked. In addition, the SIS UREs computed from observation data provide deeper insights into the SIS anomalies, such as the exact start and end epochs of the anomalies. Case studies of two interesting anomalies and the resultant receiver responses are provided at the end of the paper.

I. INTRODUCTION

With hundreds of millions of users, the NAVSTAR Global Positioning System (GPS) is so far the most widely used worldwide radionavigation system. Although GPS has proven to be a very accurate and reliable positioning service, it still exhibits a certain level of errors. One of the major error sources is the signal-in-space (SIS) user range error (URE), the pseudorange inaccuracy attributable to the ground control and the space vehicles [1], [2]. More specifically, SIS URE includes broadcast ephemeris and clock errors, satellite antenna variations [3], and signal imperfections [4], but not

ionospheric or tropospheric modeling errors, multipaths, or any errors owing to user receivers. SIS UREs are dominated by ephemeris and clock errors because antenna variations and signal imperfections are usually at a level of millimeter or centimeter [3], [4]. SIS UREs affect positioning accuracy and integrity, especially for stand-alone Standard Positioning Service (SPS) users. Normally, GPS SPS users can assume that every broadcast navigation message is reliable and a URE resulting from a healthy SIS is at meter level or even sub-meter level [5]–[8]. In practice, unfortunately, SIS anomalies occur occasionally, and UREs of tens of meters or even more have been observed. These anomalous SIS could lead to hazardous misleading position solutions for unaugmented GPS receiver [9]–[11]. Knowledge of the SIS anomalies in history has a great importance for not only assessing the GPS SIS integrity performance but also developing next generation GNSS integrity monitoring systems.

As broadcast ephemeris and clock errors dominate SIS UREs, potential SIS anomalies are typically found by comparing broadcast ephemerides and clocks with post-processed, precise ephemerides and clocks because the latter can be considered as truth [7], [12]–[17]. This method was referred as to a “bottom-up” approach in [13]; in this paper, we would like to give it a more intuitive name: “space” approach. One problem with the space approach is that false anomalies may be claimed because broadcast ephemeris/clock data obtained from a global tracking network sometimes contain errors made by receivers or data processing software [18]. These data-logging errors could result in about 10 times more false anomalies than true anomalies [14], [17]. Although we have developed a data cleansing algorithm based on majority voting to recover original broadcast navigation messages [14], [16], [17], there is still a concern of false anomalies caused by any residual data-logging errors or rare errors in precise ephemerides and clocks. Another problem with the space approach is that false anomalies may also result from a satellite indicating an unhealthy state through the use of nonstandard SIS [1], [19] because neither broadcast nor precise ephemeris and clock data include the information about the satellite

trackability. The third problem with the space approach is that the precise ephemerides and clocks are usually given at 15-minute intervals, a very low sampling rate that can hardly support a detailed and accurate depiction of the SIS anomalies.

A solution to the above three problems with the space approach is the “top-down” approach [13], referred as to a “ground” approach in this paper. In the ground approach, SIS UREs are derived from ground observation data via deducting non-SIS errors from the total pseudorange errors. However, most implementations of the ground approach required too much manual intervention, such as selecting a data source by hand and verifying an anomaly by eyes [7], [13]. In this paper, we aim at an automated process to verify the potential SIS anomalies identified in our previous papers [15]–[17] using the ground observation data from the International GNSS Service (IGS) [20].

The rest of this paper is organized as follows. Section II thoroughly describes the verification process. Section III shows the verification results and compares them with the results of the space approach. Section IV presents in-depth case studies on two interesting anomalies. Section V summarizes this paper.

II. VERIFICATION PROCESS

Fig. 1 shows the whole verification process. For each potential anomaly, the space approach in our prior work [15]–[17] has provided the following information:

- The pseudorandom noise (PRN) signal number and the space vehicle number (SVN) of the anomalous satellite;
- The start time and the duration of the anomaly with a resolution of 15 minutes;
- The broadcast and precise satellite orbits and clocks at 15-minute intervals;
- The broadcast user ranging accuracy (URA).

Accordingly, the first step in the verification process is to determine preferred IGS stations based on the above information and the coordinates of all IGS stations. Then, the GPS navigation and observation data collected by these preferred IGS stations are downloaded from an IGS archive site, Crustal Dynamics Data Information System (CDDIS) [21]. The second step is to compute the SIS UREs of the anomalous satellite

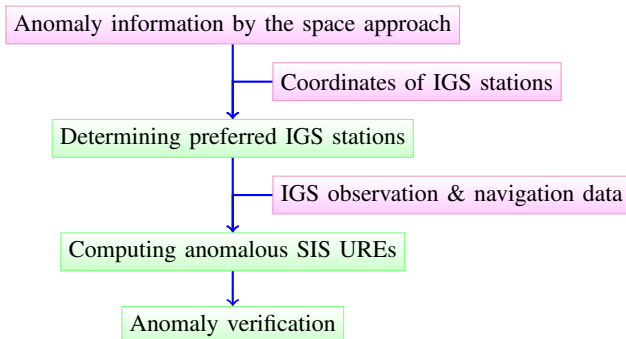


Fig. 1. The whole verification process.

via deducting non-SIS errors from the total pseudorange errors. In the last step, the SIS UREs experienced by each preferred IGS station generate a decision among “anomalous,” “normal,” and “untracked;” these independent decisions are combined to determine if the potential anomaly is true, false, untracked, or paradoxical. The whole process is fully automated, as a manual intervention is only needed when a potential anomaly is determined to be “paradoxical.”

For the rest of this section, Subsection II-A, II-B, and II-C will describe the three steps respectively.

A. Determination of preferred IGS stations

As shown in Fig. 2, the IGS tracking network is made up of more than 350 volunteer stations all over the world. A GPS satellite can usually be tracked by 30–150 stations simultaneously. In order to reduce the computational cost, for each potential anomaly our process computes the SIS UREs based on the data from 10–32 preferred stations. These stations are selected according to the following requirements:

- The station must be active when the anomaly occurred;
- The station must be in the footprints of the anomalous satellite through the whole anomaly event, or as long as possible;
- The station should experience as large anomalous SIS UREs as possible.

Among the three requirements, it is easy to meet the first one by checking the filenames in the CDDIS server. To coordinate the last two requirements, we propose a simple criterion that a station is more preferred if the sum of the absolute values of the anomalous SIS UREs observed by this station is larger. For example, supposing there was a 30-minute anomaly, and Station A experienced 15-meter and 20-meter SIS UREs for the first 15 minutes and the last 15 minutes respectively, while Station B experienced 30-meter SIS URE for the first 15 minutes but was out of the footprints of the satellite for the last 15 minutes. Then, Station A is more preferred because $15 + 20 > 30$. However, if Station B had experienced 40-meter SIS URE for the first 15 minutes only, it would have been more preferred because $15 + 20 < 40$. Although this criterion seems to be arbitrary, it is very efficient and effective in processing the real data.

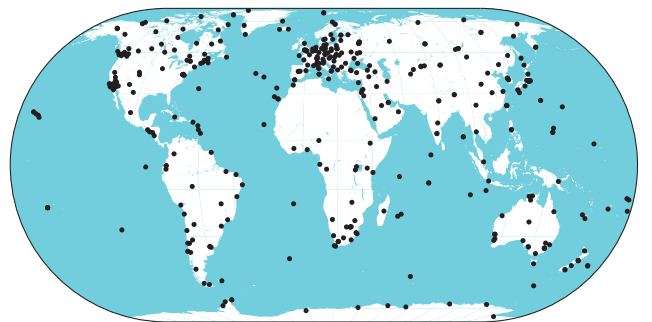


Fig. 2. IGS Tracking Network as of Mar 17, 2012 (adapted from [22])

The criterion can be implemented as follows. Assuming that we want to verify a potential GPS SIS anomaly of PRN p occurring at $\{t_1, \dots, t_n\}$ (epochs at 15-minute intervals) on Day d of the Year y , a list of preferred stations can be generated by the following algorithm.

- 1: **for all** IGS station s such that s has the GPS navigation and observation data on Day d of the Year y **do**
- 2: Assign an initial priority value of this station $w_s \leftarrow 0$
- 3: **for all** $t \in \{t_1, \dots, t_n\}$ **do**
- 4: **if** station s in the footprint of PRN p at t **then**
- 5: Compute the SIS URE e of PRN p observed by s at t {using the station latitude, longitude and elevation provided by IGS [22] and the broadcast and precise satellite orbits and clocks provided in our prior work [15]–[17]}
- 6: **if** $|e| < 4.42 \cdot \text{URA UB}$ **then**
- 7: $e \leftarrow 0$
- 8: **end if**
- 9: Update the priority value $w_s \leftarrow w_s + |e|$
- 10: **end if**
- 11: **end for**
- 12: **end for**
- 13: Sort the IGS stations in descending order for the priority values w_s

For each potential GPS SIS anomaly, the above algorithm gives a list of the IGS stations whose navigation and observation data can be used to verify the anomaly. In addition, these IGS stations are sorted from the most preferred to the least preferred. Therefore, our process sequentially downloads the receiver independent exchange (RINEX) navigation and observation data from the first 10–32 station in the list, and computes SIS UREs for each station.

B. Computation of anomalous SIS UREs

1) *Ranging error model*: For a single-frequency GPS receiver, a measured pseudorange ρ can be modeled as [23]

$$\rho = r + c(b_u - b^s) + I + T + \epsilon, \quad (1)$$

where r is the true range, c is the speed of light, b_u is the receiver clock bias, b^s is the true satellite clock bias, I is the ionospheric delay, T is the tropospheric delay, and ϵ is a composition of all unmodeled effects, modeling errors, and measurement noises except the SIS URE.

An SPS receiver typically derives real-time satellite orbits and clocks from broadcast navigation messages, the true range can be written as

$$r = \hat{r} - \epsilon_e, \quad (2)$$

where \hat{r} is the “true range” based on the broadcast ephemeris, and ϵ_e is the broadcast ephemeris error projected onto the line between the receiver and the satellite. Similarly, the true satellite clock bias can be written as

$$b^s = \hat{b}^s - \epsilon_c, \quad (3)$$

where \hat{b}^s is the broadcast satellite clock bias, and ϵ_c is the broadcast clock error.

Plugging (2) and (3) into (1), we can obtain

$$\text{SIS URE} = \epsilon_e - c\epsilon_c = \hat{r} + c(b_u - \hat{b}^s) + I + T + \epsilon - \rho. \quad (4)$$

The values on the right side of (4) can be computed or estimated as follows.

ρ	is pseudorange measured by the receiver.
\hat{r}	is the distance between the satellite position computed from the broadcast ephemeris and the estimated receiver position;
b_u	is the estimated receiver clock bias;
\hat{b}^s	is the broadcast satellite clock bias computed from the clock correction terms in the navigation message;
I	is the ionospheric delay estimated from the Klobuchar model ¹ [24];
T	is the tropospheric delay estimated from the Saastamoinen model [23];
ϵ	cannot be fully estimated, but a portion of it, the receiver code multipath, can be alleviated by a carrier smoothing.

According to [23], the total estimation error for the right side of (4) is around 5 meters. This accuracy is acceptable for the purpose of this paper because anomalous SIS UREs are always larger than 10.6 meters.

2) *Estimation of receiver position and clock biases*: The above analysis of ranging error model shows that we need the receiver position and the receiver clock biases in order to estimate the SIS UREs. Usually, a RINEX observation file provides the receiver position in its header. Unfortunately, not all IGS stations have a survey-grade receiver position in the header of their RINEX files. In this paper, we use the following method to cope with this problem: (1) estimate the receiver position from the observation data; (2) if the estimated receiver position is within 5 meters of the receiver position given by the header of the RINEX file, then use the given receiver position, otherwise use the estimated receiver position.

Since the receivers in IGS network are usually static, a receiver position can be accurately estimated by averaging many position estimates. In this paper, we estimate a receiver position using three days of data around the day when the anomaly occurred. To avoid any interference due to outliers, not only is the anomalous satellite excluded in the computation, but a 10% trimmed mean² is also used to average the position estimates.

With a known receiver position \mathbf{x} , the pseudoranges obtained after accounting for satellite clock bias, ionospheric delay, tropospheric delay, and multipath can be modeled as

¹Although dual-frequency pseudorange measurements can provide a better estimation of the ionospheric delay, this paper prefers a single-frequency-based model because (1) the GPS SPS performance standard [1] is defined only for L1 C/A, and (2) the semi-codeless/codeless L2 P(Y) pseudorange measurements are usually more noisy and less reliable than the L1 C/A measurements.

²Also referred to as truncated mean. A 10% trimmed mean is the mean after discarding the samples at the 5% high end and 5% low end. In fact, as a robust estimator of central tendency, the trimmed mean is a compromise between a mean and a median.

[23]

$$\tilde{\rho}^{(k)} = \|\mathbf{x}^{(k)} - \mathbf{x}\| + b_u + \tilde{\epsilon}^{(k)}, \quad (5)$$

where $k = 1, \dots, K$ is the index of the K available satellites at this epoch (excluding the anomalous satellite), and $\mathbf{x}^{(k)}$ is the satellite position. A minimum-mean-square-error estimator of b_u is given by the weighted mean

$$b_u = \frac{1}{\sum_{k=1}^K w_k} \sum_{k=1}^K w_k (\tilde{\rho}^{(k)} - \|\mathbf{x}^{(k)} - \mathbf{x}\|), \quad (6)$$

where the weights $w_k = 1/\text{var}(\tilde{\epsilon}^{(k)})$ can be derived from the signal-to-noise (SNR) ratio, satellite elevations, etc. using the algorithms described in [23], [25].

C. Verification of anomalies

In this paper, a GPS SIS anomaly is defined as a threat of an GPS SIS integrity failure [1], [16], [17]. Accordingly, an anomalous GPS SIS behavior is defined as a fulfillment of all the following conditions:

- The SIS URE exceeds 4.42 times the upper bound (UB) on the broadcast URA [1], [26];
- The broadcast navigation message is healthy, i.e.,
 - The RINEX field `SV_health` [27] is 0, and
 - The URA UB ≤ 48 meters [1];
- The time of transmission is in the fit interval of the navigation message [26];
- The L1 C/A signal was tracked with a reasonable SNR [1].

Similarly, a normal GPS SIS behavior is decided when the last condition is fulfilled but any of the first three conditions is not. When the L1 C/A signal was not tracked with a reasonable SNR, the decision is “untracked” because (1) the SIS might be normal as the satellite could indicate an unhealthy state through ceasing transmission or using nonstandard code or data [1], [19], or (2) the SIS might be anomalous as the satellite could be blocked by a build-in integrity monitoring function of the receiver. Therefore, for each potential GPS SIS anomaly, the observation and navigation data from one IGS station give one of the three decisions: anomalous, normal, and untracked.

As mentioned in Subsection II-A, each potential GPS SIS anomaly are verified by checking the RINEX observation and navigation data from 10–32 preferred IGS stations. Because the data from each of these stations give an independent decision, the final verification decision is made by merging the 10+ independent decisions. Table I shows the decision table that our process uses to combine these independent decisions.

According to Table I, a potential GPS SIS anomaly is proven to be “true” if the observation data from at least one of the 10+ preferred IGS stations show anomalous SIS UREs while the rest stations could not track the satellite during the anomaly event. Similarly, a potential anomaly is proven to be “false” if the observation data from at least one of the 10+ stations show normal SIS UREs while the rest could not track the satellite. An “untracked” decision is made when

TABLE I
DECISION TABLE TO MERGE THE INDEPENDENT DECISIONS INTO THE FINAL VERIFICATION DECISION

Final decision	Number of IGS stations that decide		
	Anomalous	Normal	Untracked
True	≥ 1	$= 0$	≥ 0
False	$= 0$	≥ 1	≥ 0
Untracked	$= 0$	$= 0$	≥ 10
Paradoxical	≥ 1	≥ 1	≥ 0

no IGS stations in the footprints of the anomalous satellite could track the satellite; the anomaly is, although not *proven* to be false, *most likely* to be false. Besides, a “paradoxical” decision is made when some IGS stations show anomalous SIS UREs and some show normal. Our process can alert us to check a “paradoxical” manually. This is the only case in which a manual intervention is needed. Fortunately, we have not encountered any “paradoxical” in this paper.

III. VERIFICATION RESULTS

We apply the automated verification process to the 31 potential GPS SIS anomalies³ during the past eight years⁴ found in our prior work [15]–[17]. Table II shows a side-by-side comparison of the verification results with our prior results found by the space approach. It can be seen that

- 26 potential anomalies have been verified to be true;
- 1 potential anomalies have been verified to be false because the satellite was normally tracked with SIS UREs smaller than 3 meters;
- 4 potential anomalies are most likely to be false because they were not tracked through the whole anomaly event.

These results show that our prior work is of great value. Moreover, the number of true SIS anomalies per year demonstrates excellent GPS SIS integrity performance in the past 4 years, much better than that before 2008.

It should be noted that for a certain SIS anomaly, different stations may observe different anomalous SIS URE behaviors. For each of the 26 true anomalies and the false anomaly, the values of start time, duration, and maximum SIS URE in the verification results of Table II are based on the RINEX data from the station listed in the “Reference” column.

Comparing the verification results of the 26 true anomalies with our prior results, we can see that the anomaly start time or duration derived from the ground approach sometimes disagree with those from the space approach. One of the reasons is that the IGS daily observation data are recorded at a sample interval of 30 seconds, while the precise ephemerides and clocks used in the space approach are usually given at 15-minute intervals. The different sampling frequencies naturally cause that the start time given by the ground approach is earlier than that

³The clock anomaly of Space Vehicle Number (SVN) 23/PRN 23 occurred on Jan 1, 2004 [11], [28] was missed by our process in [15]–[17] because the IGS precise clocks for PRN 23 on that day were absent. The values such as start time, duration, and maximum SIS URE for this potential anomaly in Table II are derived from a comparison with the precise ephemerides and clocks from the Center for Orbit Determination in Europe (CODE).

⁴No potential GPS SIS anomaly was found for 2011.

TABLE II
VERIFICATION RESULTS COMPARED WITH OUR PRIOR RESULTS

Potential anomalies found in our prior work via space approach						Verification result in this paper via ground approach								
SVN	PRN	Date	Start Time	Duration (minutes)	Anomaly	Max URE (meters)	URA UB (meters)	Start Time	Duration (minutes)	Max URE (meters)	Reference	Number of stations that decide		
												Anomalous	Normal	Untracked
23	23	2004/01/01	18:45:00	165	clock	284000	2.40	18:31	169	298600	bhr1	5	0	5
38	8	2004/04/22	13:15:00	90	clock	29	4.85	13:07	32	29.5	qui1	2	0	11
38	8	2004/05/03	11:15:00	15	clock	-30.2	3.40	10:58	19	-32.86	bue1	3	0	10
38	8	2004/05/05	08:30:00	60	clock	-29.5	2.40	08:23	34	-35.18	eil1	3	0	10
29	29	2004/06/17	11:15:00	105	ephemeris	13	2.40	11:09	48	13.26	wel2	2	0	8
60	23	2004/07/20	07:15:00	45	ephemeris	13	2.40	06:31	73	17.35	suth	13	0	3
27	27	2004/08/29	00:45:00	120	clock	70.4	3.40	00:42	160	71.5	brmu	11	0	5
27	27	2005/05/14	20:15:00	90	clock	116	2.40	20:01	18	31.63	gmsd	12	0	4
26	26	2005/06/09	03:45:00	60	clock	-37.9	3.40	03:38	17	-35.24	irkj	14	0	2
25	25	2005/12/25	21:15:00	60	clock	2050	2.40	21:05	25	-174	osn2	14	0	2
30	30	2006/06/02	20:30:00	30	clock	1045	2.40	20:04	11	160	mas1	15	0	0
36	6	2006/06/27	04:45:00	30	clock	-10.8	2.40	04:42	29	-11.39	mcm4	16	0	0
33	3	2006/07/31	22:15:00	60	clock	-12.7	2.40	22:13	51	-13.14	hrm1	16	0	0
29	29	2006/08/25	12:30:00	90	clock	-11.6	2.40	12:24	95	-11.85	sey1	16	0	0
24	24	2006/09/22	19:45:00	165	ephemeris	41.2	2.40	19:54	22	12.78	mcm4	7	0	9
35	5	2006/11/07	01:45:00	225	clock	-30.7	2.40	01:44	31	-17.93	tah2	15	0	1
29	29	2007/03/01	14:45:00	150	clock	-42.3	2.40	14:38	8	-13.01	faa1	8	0	8
54	18	2007/04/10	16:00:00	105	ephemeris	688	2.40	16:04	61	398	tah2	13	0	3
59	19	2007/05/20	03:45:00	15	ephemeris	-13.3	2.40		false anomaly	-2.42	uclu	0	17	0
37	7	2007/08/17	07:30:00	30	clock	-14.3	2.40	07:22	38	-16.24	jplm	16	0	0
58	12	2007/10/08	09:45:00	135	clock	-86000	2.40		satellite was not tracked			0	0	23
41	14	2007/10/08	23:00:00	90	clock	-112000	2.40		satellite was not tracked			0	0	32
60	23	2007/10/09	09:45:00	60	clock	27000	6.85	09:53	46	26650	tid2	5	0	11
56	16	2007/10/09	13:15:00	15	clock	-18000	4.85	12:55	37	-18450	nr11	6	0	9
51	20	2007/10/10	08:45:00	75	clock	48000	2.40	09:06	47	47690	osn1	6	0	10
27	27	2008/11/14	05:45:00	225	clock	-69800	2.40		satellite was not tracked			0	0	32
25	25	2009/06/26	09:30:00	45	clock	-22.3	2.40	09:05	40	-22.42	guao	15	0	0
38	8	2009/11/05	18:45:00	30	clock	-18.5	2.40	18:40	22	-18.32	bue1	15	0	1
30	30	2010/02/22	21:00:00	30	clock	-42.9	3.40	20:46	5	-15.3	areq	14	0	2
39	9	2010/04/25	19:45:00	15	ephemeris	11	2.40	19:31	29	11.65	xian	9	0	1
56	16	2010/06/24	18:30:00	120	clock	374	2.40		satellite was not tracked			0	0	29

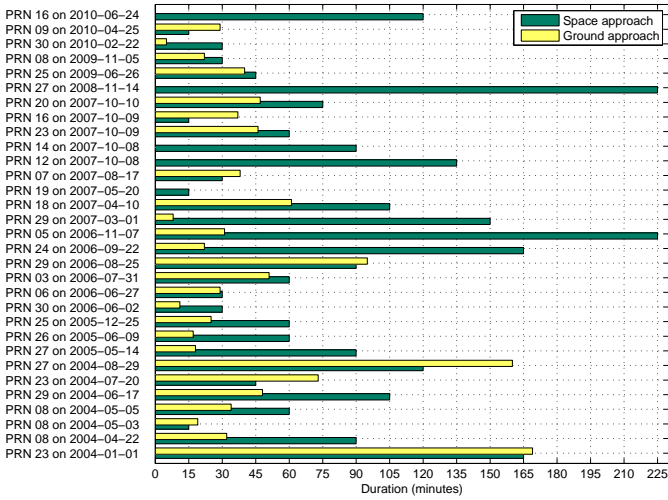


Fig. 3. Duration of the GPS SIS anomalies. For nearly half of the true anomalies, the duration given by the ground approach is significantly shorter than that by the space approach.

by the space approach, and the duration given by the ground approach is longer than that by the space approach.

Nevertheless, Fig. 3 shows that, for nearly half of the true anomalies, the duration given by the ground approach is significantly shorter than that by the space approach. The reason is that, when a SIS anomaly is detected by the satellite or the ground control, a GPS satellite may alert the users by cease transmitting L1 signal or using nonstandard code or data [1], [19] before updating the navigation messages. In fact, half of the true anomalies ended with the receivers losing track of the anomalous satellites. In the space approach, due to the lack of the information about the signal trackability, the end of an anomaly is usually the instant when the anomalous navigation message expires or an updated navigation message was issued. Therefore, the anomaly duration given by the space approach may be longer than the fact.

The last apparent disagreement between the ground approach and the space approach is the maximum SIS URE. One reason for this disagreement is that, as just mentioned, an anomaly might end earlier than the space approach thought, and the SIS UREs did not actually grow to as a large value as the space approach found. Another reason is that the maximum SIS URE in the ground approach are affected by meter-level estimation errors.

IV. CASE STUDIES

This section presents in-depth case studies of the SVN 29/PRN 29 anomaly on Mar 1, 2007 and the SVN 33/PRN 03 anomaly on Jul 31, 2006. We selected the SVN 29 anomaly because its duration given by the ground approach is significantly shorter than that by the space approach. We selected the SVN 33 anomaly because not only it is one of only a few anomalies that was not notified via the Notice Advisory to NAVSTAR Users (NANU) [16], [17], but it also led to various receiver responses.

A. SVN 29/PRN 29 anomaly on Mar 1, 2007

Fig. 4 shows the SIS UREs (blue dots) of SVN 29 computed from the observation data of the IGS station *faa1*, compared with the SIS UREs given by the space approach (red circles). We can see that the SIS UREs computed by the ground approach highly match those computed by the space approach. The ground approach shows that the anomaly started at 14:38, when the SIS UREs exceeded 4.42 URA UB, and ended at 14:46, when the satellite became untrackable. Therefore, the anomaly lasted for only 8 minutes. At 17:07, the satellite became trackable again and started to broadcast a new navigation message with an unhealthy flag. The space approach gave a duration of 150 minutes for this anomaly because, without the information about the satellite trackability, it thought that the anomaly started at 14:45 and ended at 17:15.

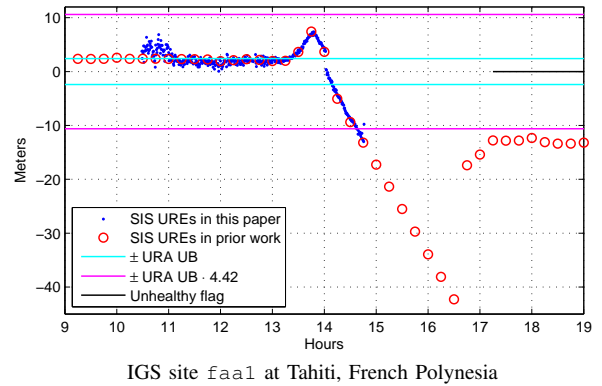


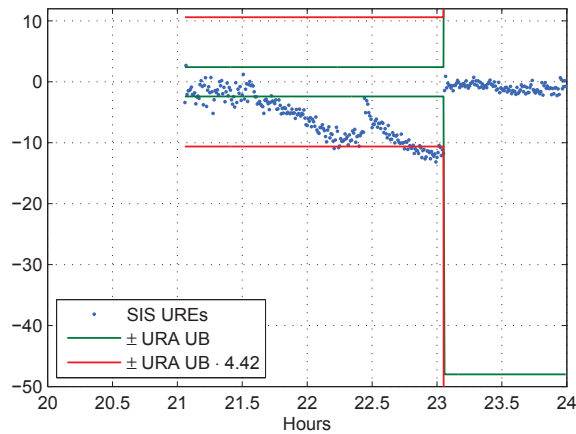
Fig. 4. SIS UREs of SVN 29/PRN 29 on Mar 1, 2007.

B. SVN 33/PRN 03 anomaly on Jul 31, 2006

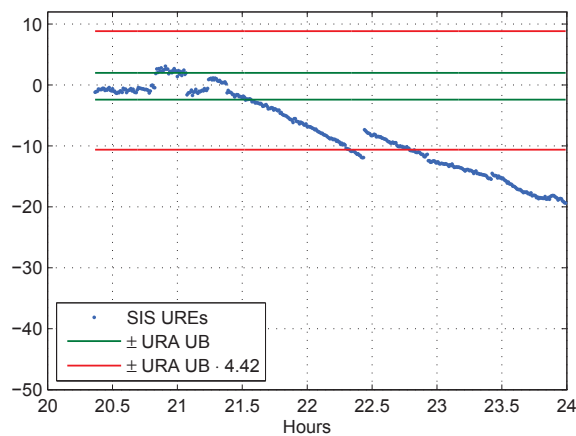
Fig. 5 shows the SIS UREs of SVN 33 observed by two IGS stations, *hrml* and *kuuj*. The anomaly experienced by *hrml* started at 22:13 and ended at 23:04, when a new navigation message with a 48-meter URA UB was broadcast (ironically, this navigation message led to the SIS UREs around 2 meters). Accordingly, the maximum SIS URE that *hrml* experienced was 13.14 meters, very close to the value given by the space approach (see Table II).

In contrast, *kuuj* experienced a very different story because it did not receive the new navigation message with the 48-meter URA UB. The SIS anomaly started at 22:20 but lasted till midnight, culminating in a SIS URE of 19.38 meters. The observation data show that *kuuj* kept tracking the satellite since 20:22; it is unclear why *kuuj* missed the new navigation message.

In order to know if there are any other receivers having the same problem as *kuuj*, we screened all the navigation data collected by the IGS network on Jul 31, 2006. To our surprise, among the 245 IGS stations that were tracking PRN 03 around 23:00, 29 stations missed the new navigation message. Although the navigation message handover problem may occur very rarely, it implies that it is probably a more



(a) IGS site hrml at Hermitage, West Berkshire, UK



(b) IGS site kuuj at Kuujuaarapik, QC, Canada

Fig. 5. SIS UREs of SVN 33/PRN 03 on Jul 31, 2006.

timely and reliable way to alert users via making the satellite untrackable than issuing a new navigation message.

V. SUMMARY

In this paper, we developed an automated process to verify potential GPS SIS anomalies using the IGS ground observation data. Given the basic information about each potential anomaly, our process can automatically select 10–32 preferred IGS stations, retrieve their observation and navigation data, compute SIS UREs, and decide if the potential anomaly is true. We apply this process to the 31 potential GPS SIS anomalies found from Jan 1, 2004 to Dec 31, 2011. The results show that 26 potential anomalies are true, 1 is false, and 4 are untracked. Moreover, the number of true SIS anomalies per year demonstrates an improving SIS integrity performance over the past eight years. A comparison between the verification results and our prior results shows that the SIS UREs computed from observation data provide more accurate information and deeper insights of the anomalous SIS behaviors, especially when an anomaly was ended by making the anomalous satellite untrackable. We also studied the SVN 29/PRN 29 anomaly on Mar 1, 2007 and the SVN 33/PRN 03 anomaly on Jul 31, 2006.

Our case studies show that an unexpected anomaly can appear when a receiver misses a navigation message. We hope that the results presented in this paper will help not only numerous GPS users but also the development of next generation GNSS integrity monitoring systems.

ACKNOWLEDGMENT

The authors gratefully acknowledge the support of the Federal Aviation Administration under Cooperative Agreement 08-G-007. This paper contains the personal comments and beliefs of the authors, and does not necessarily represent the opinion of any other person or organization.

REFERENCES

- [1] US DoD, *Global Positioning System Standard Positioning Service Performance Standard*, 4th ed., September 2008.
- [2] K. Kovach, “New user equivalent range error (URE) budget for the modernized Navstar Global Positioning System (GPS),” in *Proceedings of the 2000 National Technical Meeting of The Institute of Navigation (NTM 2000)*, Anaheim, CA, January 2000, pp. 550–573.
- [3] R. Schmid, M. Rothacher, D. Thaller, and P. Steigenberger, “Absolute phase center corrections of satellite and receiver antennas,” *GPS Solutions*, vol. 9, pp. 283–293, 2005.
- [4] R. E. Phelts, G. X. Gao, G. Wong, L. Heng, T. Walter, P. Enge, S. Erker, S. Thoelet, and M. Meurer, “Aviation grade: New GPS signals—chips off the Block IIF,” *Inside GNSS*, vol. 5, no. 5, pp. 36–45, July 2010.
- [5] R. B. Langley, H. Jannasch, B. Peeters, and S. Bisnath, “The GPS broadcast orbits: an accuracy analysis,” in *33rd COSPAR Scientific Assembly*, Warsaw, Poland, July 2000.
- [6] D. M. Warren and J. F. Raquet, “Broadcast vs. precise GPS ephemerides: a historical perspective,” *GPS Solutions*, vol. 7, pp. 151–156, 2003.
- [7] C. Cohenour and F. van Graas, “GPS orbit and clock error distributions,” *NAVIGATION*, vol. 58, no. 1, pp. 17–28, Spring 2011.
- [8] B. Gruber, “GPS modernization and program update,” in *Stanford’s 2010 PNT Challenges and Opportunities Symposium*, Stanford, CA, November 2010.
- [9] N. Vary, “DR# 55: GPS satellite PRN18 anomaly affecting SPS performance,” FAA William J. Hughes Technical Center, Pomona, New Jersey, Tech. Rep., April 2007.
- [10] T. Walter, P. Enge, J. Blanch, and B. Pervan, “Worldwide vertical guidance of aircraft based on modernized gps and new integrity augmentations,” *Proceedings of the IEEE*, vol. 96, no. 12, pp. 1918–1935, December 2008.
- [11] D. Last, “GNSS: The present imperfect,” *Inside GNSS*, vol. 5, no. 3, pp. 60–64, May 2010.
- [12] J. Lee, “Results on test of URA validation protocol using NGA data,” in *GEAS Working Group*, May 2009.
- [13] G. X. Gao, H. Tang, J. Blanch, J. Lee, T. Walter, and P. Enge, “Methodology and case studies of signal-in-space error calculation top-down meets bottom-up,” in *Proceedings of the 22nd International Technical Meeting of the Satellite Division of the Institute of Navigation (ION GNSS 2009)*, Savannah, GA, September 2009, pp. 2824–2831.
- [14] L. Heng, G. X. Gao, T. Walter, and P. Enge, “GPS ephemeris error screening and results for 2006–2009,” in *Proceedings of the 2010 International Technical Meeting of the Institute of Navigation (ION ITM 2010)*, San Diego, CA, January 2010, pp. 1014–1022.
- [15] —, “GPS signal-in-space anomalies in the last decade: Data mining of 400,000,000 GPS navigation messages,” in *Proceedings of the 23rd International Technical Meeting of the Satellite Division of the Institute of Navigation (ION GNSS 2010)*, Portland, OR, September 2010, pp. 3115–3122.
- [16] —, “Digging into GPS integrity: Charting the evolution of signal-in-space performance by data mining 400,000,000 navigation messages,” *GPS World*, vol. 22, no. 11, pp. 44–49, November 2011.
- [17] —, “GPS signal-in-space integrity performance evolution in the last decade: Data mining 400,000,000 navigation messages from a global network of 400 receivers,” *IEEE Transactions on Aerospace and Electronic Systems*, accepted for publication.

- [18] D. C. Jefferson and Y. E. Bar-Sever, "Accuracy and consistency of broadcast GPS ephemeris data," in *Proceedings of the 13th International Technical Meeting of the Satellite Division of the Institute of Navigation (ION GPS 2000)*, Salt Lake City, UT, September 2000, pp. 391–395.
- [19] B. C. Barker and S. J. Huser, "Protect yourself! Navigation payload anomalies and the importance of adhering to ICD-GPS-200," in *Proceedings of the 11th International Technical Meeting of the Satellite Division of the Institute of Navigation (ION GPS 1998)*, Nashville, TN, September 1998, pp. 1843–1854.
- [20] J. M. Dow, R. E. Neilan, and C. Rizos, "The International GNSS Service in a changing landscape of global navigation satellite systems," *Journal of Geodesy*, vol. 83, pp. 689–689, 2009.
- [21] CDDIS, Accessed March 2012. [Online]. Available: http://igsb.jpl.nasa.gov/components/dcnav/cddis_data_daily_yn.html
- [22] IGS Tracking Network, Accessed March 2012. [Online]. Available: <http://igsb.jpl.nasa.gov/network/netindex.html>
- [23] P. Misra and P. Enge, *Global Positioning System: Signals, Measurements, and Performance*, 2nd ed. Lincoln, MA: Ganga-Jamuna Press, 2006.
- [24] J. Klobuchar, "Ionospheric effects on GPS," in *Global Positioning System: Theory and Applications*, B. Parkinson, J. Spilker, P. Axelrad, and P. Enge, Eds. Washington, DC: American Institute of Aeronautics and Astronautics, 1996, vol. I, pp. 485–515.
- [25] M. Choi, J. Blanch, D. Akos, L. Heng, G. Gao, T. Walter, and P. Enge, "Demonstrations of multi-constellation Advanced RAIM for vertical guidance using GPS and GLONASS signals," in *Proceedings of the 24th International Technical Meeting of the Satellite Division of the Institute of Navigation (ION GNSS 2011)*, Portland, OR, September 2011, pp. 3227–3234.
- [26] GPS Wing, *Interface Specification IS-GPS-200E*, June 2010.
- [27] IGS formats, Accessed January 2012. [Online]. Available: <http://igsb.jpl.nasa.gov/components/formats.html>
- [28] J. W. Lavrakas, "GPS anomaly summary," unpublished.